https://doi.org/10.5194/amt-2024-151
Preprint. Discussion started: 4 November 2024

Atmospheric Measurement Techniques Discussions

Correcting for water vapor diffusion in air bag samples for isotope composition analysis: cases studies with drone-collected samples

Di Wang[1,2,3*], Camille Risi[2], Lide Tian[1], Di Yang[1], Gabriel J. Bowen[4], Siteng Fan[2,5], Yang Su[6] , Hongxi Pang[7], Laurent Z.X Li[2]

[1] *Institute of International Rivers and Eco-security, Yunnan University, Yunnan Key Laboratory of International Rivers and Transboundary Eco–security, Kunming 650500, Yunnan, China*

[2] *Laboratoire de Météorologie Dynamique, IPSL, CNRS, Sorbonne Université, Campus Pierre et Marie Curie, Paris 75005, France*

[3] *Laboratoire Atmosphères, Observations Spatiales, IPSL, CNRS, UVSQ, Sorbonne Université, Guyancourt, France*

[4] *Department of Geology and Geophysics, University of Utah, Salt Lake City, Utah 84108, USA*

[5] *Department of Earth and Space Sciences, Southern University of Science and Technology, Shenzhen 518055, China*

[6] *Département d'Informatique, École normale supérieure – PSL, 45 Rue d'Ulm, 75005 Paris, France*

[7] *Key Laboratory of Coast and Island Development of Ministry of Education, School of Geography and Ocean Science, Nanjing University, Nanjing 210023, China*

**Corresponding author: di.wang@lmd.ipsl.fr*

https://doi.org/10.5194/amt-2024-151
Preprint. Discussion started: 4 November 2024

Atmospheric Measurement Techniques Discussions

Abstract

Traditional methodologies, such as mass spectrometry and laser spectroscopy, have been widely employed for precise water vapor isotope measurements. Nevertheless, these techniques are limited by logistical challenges in fieldwork, consequently constraining the temporal and spatial resolution of measurements. Specifically, water vapor isotope measurements are primarily limited to near-surface levels, while measurements associated with processes aloft connecting tropospheric water vapor to surface precipitation are notably scarce. Portable sampling devices, such as air bags and glass bottles, have therefore become necessary alternatives for collecting, storing, and transporting gaseous samples in diverse environments prior to analysis with less portable instruments. In drone-based high-altitude vapor sampling, air bags are preferred for their lighter weight and greater flexibility compared to glass bottles. Nevertheless, they present specific challenges, such as potential sample contamination and isotopic fractionation during storage, primarily due to the inherent permeability of air bags. Here, we developed a theoretical model for water vapor diffusion through the sampling bag surface, with parameters calibrated through laboratory experiments. This model enables the reconstruction of the initial isotopic composition of sampled vapor based on measurements obtained within the bag and from the surrounding environment. This diffusion model underwent rigorous validation through experiments conducted under diverse conditions, confirming its reliability. We applied this correction method to air samples collected at various pressures up to the upper troposphere using an air bag-mounted drone that we developed, thereby estimating the initial isotopic composition and uncertainty based on our observations. The corrected observations closely match the Picarro direct observations and IASI satellite data. Our correction method significantly enhances the reliability and applicability of water vapor isotope observations conducted using drones equipped with air bags. This approach leverages the strengths of drone-based air bag sampling while mitigating its limitations, thus facilitating the convenient collection of isotopic data throughout the troposphere.

https://doi.org/10.5194/amt-2024-151
Preprint. Discussion started: 4 November 2024

Atmospheric Measurement Techniques Discussions

1 Introduction

Water vapor isotopes provide unique insights into the transport, mixing, and phase changes of water in the environment, which are crucial for improving understanding of the climate system, hydrological cycle, atmospheric dynamics, and paleoclimate proxies. Water isotopes have also been applied in climate modeling, weather prediction, and water resource management (Bowen et al., 2019; Galewsky et al., 2016; Gat, 1996; West et al., 2009).

Water isotope analysis has traditionally relied on mass spectrometry, which, while accurate (Ghosh and Brand, 2003; Muccio and Jackson, 2009), demands labor-intensive preparation and lacks portability (West et al., 2010). Methods like cryogenic trapping effectively collect water vapor (Grootes and Stuiver, 1997; Michener and Lajtha, 2008; Steen-Larsen et al., 2011; Yu et al., 2015) , but they require long sampling periods, limiting observation scope and timing. Over the past three decades, laser spectroscopy methods such as Cavity Ring-Down Spectroscopy (CRDS)(Hodges and Lisak, 2006) and Off-Axis Integrated Cavity Output Spectroscopy (OA-ICOS) (Johnson et al., 2011) have emerged, delivering a best-in-class combination of speed, high precision, and continuous measurements even in challenging environments such as high altitudes or arid regions with low water vapor content. Advances in these instruments have significantly expanded the field of water isotope research. However, their heavy instrumentation, substantial power requirements, and limited mobility restrict their usability in certain situations. As a result, the collection and storage of physical samples are still necessary, increasing the demand for more convenient and efficient sample acquisition methods. Air bags and glass bottles have been practical solutions for collecting, storing, and transporting gaseous samples from various settings (Jiménez-Rodríguez et al., 2019; Rozmiarek et al., 2021).

Given that air bags can reduce the weight of sampling equipment and increase sampling flexibility, there is considerable interest in using them for vapor sample collection. This is particularly advantageous for small equipment like drones, where minimizing payload weight is essential for sampling at high altitudes or over long distances. This selection also makes it easier to transport samples and reduces the risk of breakage. However, concerns have arisen regarding the suitability of various sampling materials for storing these samples, primarily due to potential water diffusion through container walls. Diffusion issues are commonly observed in sampling bags during water vapor isotope analysis and have persisted as a longstanding challenge in the field (Herbstritt et al., 2023; Jiménez-Rodríguez et al., 2019). In previous studies, this issue is particularly concerning in the Direct Vapor Equilibrium Laser Spectroscopy (DVE-LS) method, which has been widely used to rapidly collect and measure water isotopes in evaporation-prone soil, rock, or plant samples. The DVE-LS method simplifies preparation and increases sample throughput by directly analyzing the vapor phase, thus eliminating the need for extensive physical extractions (Gralher et al., 2021; Hendry et al., 2015; Millar et al., 2018; Sprenger et al., 2015; Wassenaar et al., 2008). However, water vapor molecules may exchange between the air inside the bag and the external ambient air during sample storage. Water vapor molecules typically diffuse from areas of high humidity to drier areas. In this process, heavier isotopes (e.g., $H_2{}^{18}O$ and HDO) move more slowly than lighter isotopes (e.g., $H_2{}^{16}O$) due to their greater mass, resulting in preferential diffusion of lighter isotopes. This selective diffusion, known as fractionation, can alter the original isotopic

https://doi.org/10.5194/amt-2024-151
Preprint. Discussion started: 4 November 2024

Atmospheric Measurement Techniques Discussions

composition of the collected air samples.

To mitigate these issues, materials with lower permeability are suggested for water vapor isotope measurements (Herbstritt et al., 2023). Further research and development are still necessary. This may involve exploring alternative materials for more impermeable sampling bags, improving sealing methods to better isolate sampled air, and developing sampling techniques less susceptible to diffusion. Resolving these issues is essential for ensuring the reliability of water vapor isotope measurements using air bags and for accurately understanding atmospheric and hydrological processes.

In light of the ongoing development and further refinement of these techniques and the associated cost constraints, we developed a diffusion model with parameters calibrated through laboratory experiments. This model is capable of assessing the permeability of the air bags and correcting the obtained isotope values to the initial pre-diffusion values based on the humidity, isotope values inside and outside the bag, and the sample storage time. This diffusion model was validated through experiments under diverse conditions, confirming its reliability. Furthermore, we also applied this diffusion method to air samples collected at different altitudes using a drone-based atmospheric vapor sampling device we developed, to estimate the initial isotope composition and uncertainty. The primary objective of this drone-based field campaign is to obtain atmospheric water vapor isotope data along vertical profiles in the troposphere, providing higher temporal and spatial resolution than satellite observations. The corrected data for drone-based measurements using our diffusion model show consistency with Picarro direct observations and satellite data, further confirming the model's theoretical and practical reliability in applications.

2 Theoretical basis of diffusion model

2.1 Diffusion model description

Storing vapor samples in air bags prior to isotope measurement may alter the isotopic composition of the water vapor. The main reason is the diffusion of water molecules between the interior and exterior of the air bags, primarily due to the permeability of the bag materials. We present a mathematical model for the diffusion and fractionation of isotopes across the surface of the sampling bag. In this model, we assume the ambient vapor flux entering the air bag changes the internal humidity and vapor isotope values, influenced by the different humidity and water isotope values inside and outside the bag (Fig.1). Note that we use isotope ratios (R) in the following equations for mathematical convenience and conciseness, but present isotope values δ in figures in subsequent sections for visualization purposes.

The flux of water toward the bag, F, is expressed as:

$$F = k * (q_e - q(t)) \quad (1)$$

where q(t) represents the variation of humidity inside the air bag over time (in g/kg), q_e denotes the environmental humidity (in g/kg), and k is a constant (in kg/m^2/s)

Similarly, the flux of isotopologue, F_i, either $H_2{}^{18}O$ or HDO, moving toward the bag can be described as:

$$F_i = k_i * (R_e * q_e - R(t) * q(t)) \quad (2)$$

https://doi.org/10.5194/amt-2024-151
Preprint. Discussion started: 4 November 2024

Atmospheric Measurement Techniques Discussions

In this equation, k_i represents a constant specific to each isotopologue, R_e denotes the isotopic ratio in the environment, and R(t) is the variation of isotopic ratio within the air bag with time. Notably, the fractionation coefficient can be denoted by $\alpha=\frac{k}{k_i}$.

The temporal change in humidity can be modeled by the following differential equation:

$$\frac{d(q(t)*M)}{dt} = F * A \quad (3)$$

where A represents the exchange area (surface area of the air bag), and M is the air mass inside the bag.

If M is constant, this equation simplifies to:

$$\frac{dq(t)}{dt} = \frac{F*A}{M} = \frac{k*A}{M} * (q_e - q(t)) \quad (4)$$

Here, we define the diffusion coefficient of humidity, $\frac{k*A}{M}$, as λ.

Similarly, the temporal change in isotopic ratio can be modeled by the following differential equation:

$$\frac{d(R(t)*q(t)*M)}{dt} = M * (q(t) * \frac{dR(t)}{dt} + R(t) * \frac{dq(t)}{dt})$$

$$= F_i * A = k_i * (R_e * q_e - R(t) * q(t)) * A \quad (5)$$

This equation can be simplified as:

$$\frac{dR(t)}{dt} = \frac{ki*(R_e*q_e - R(t)*q(t))*A/M - R(t)*\frac{dq(t)}{dt}}{q(t)}$$

$$= \frac{\frac{k*A}{M*\alpha}*(R_e*q_e - R(t)*q(t)) - R(t)*\frac{k*A}{M}*(q_e - q(t))}{q(t)}$$

$$= \frac{\frac{\lambda}{\alpha}*(R_e*q_e - R(t)*q(t)) - R(t)*\lambda*(q_e - q(t))}{q(t)} \quad (6)$$

The differential equation for humidity (Eq. 4) can be analytically solved :

$$q_e - q(t) = (q_e - q_0) * e^{(-\frac{k*A}{M}*t)} = (q_e - q_0) * e^{(-\lambda*t)} \quad (7)$$

where q_0 is the initial humidity at t = 0. This equation can also be expressed in terms of natural logarithms as:

$$\ln(q_e - q(t)) = \ln(q_e - q_0) - \lambda * t \quad (8)$$

Consequently, the slope of $\ln(q_e - q(t))$ against time is λ.

For the isotopic ratio, the analytical solution is only feasible when the initial humidity equals the environmental humidity ($q_0 = q_e$) :

$$\frac{dR(t)}{dt} = \frac{k*A}{M*\alpha} * (R_e - R(t)) \quad (9)$$

Thus, $R_e - R(t) = (R_e - R_0) * e^{(-\frac{k*A}{M*\alpha}*t)}$ (10)

where R_0 denotes the initial isotopic ratio at t = 0. Again, taking the natural logarithm, we obtain:

https://doi.org/10.5194/amt-2024-151
Preprint. Discussion started: 4 November 2024

Atmospheric Measurement Techniques Discussions

$$\ln(R_e - R(t)) = \ln(R_e - R_0) - \frac{\lambda}{\alpha} * t \quad (11)$$

This equation demonstrates that the slope of $\ln(R_e\text{-}R(t))$ against time is the diffusion coefficient of isotopic ratio $\frac{\lambda}{\alpha}$. Knowing λ, we can deduce the isotopic fractionation coefficient, α, for each isotope.

However, when the environmental humidity differs from the initial humidity inside the air bag, a numerical solution is required to solve the differential equation for R (Eq. 6).

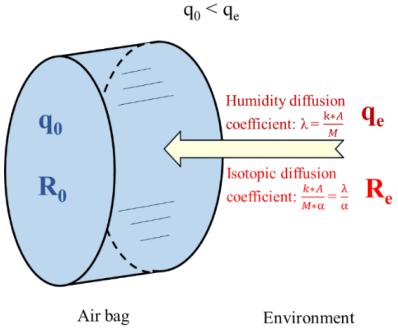

Figure 1 Schematic illustrating the diffusion model. q_0 *represents the initial humidity in the air bag at t = 0,* q_e *denotes the environmental humidity,* R_0 *indicates the initial isotopic ratio in the air bag at t = 0,* R_e *represents the isotopic ratio in the environment, k is a constant, A denotes the exchange area (surface area of the bag), and M is the mass of air within the bag, and α denotes the isotopic fractionation coefficient.*

2.2 Reconstructing initial water vapor isotopic compositions

The isotopic composition of the air bag water vapor undergoes an exponential evolution over time (Eq. 10). This method of applying exponential evolution equations to reconstruct isotopic compositions has been used in environmental forensics to investigate shifts in water isotopes due to metabolic changes, environmental conditions, or diet (Ayliffe et al., 2004; Cerling et al., 2006). Similarly, in climatology, this method helps retrieving initial isotopic values from samples such as ice cores or tree rings, affected by evaporation, precipitation, and temperature fluctuations, facilitating historical climate reconstruction (Brienen et al., 2016). Here we apply a similar method, and apply the analytical solution of Equation 6 using data from experiments in which the condition that q_0 equals q_e is met to determine the equation parameters.

The constants (λ, $\alpha\_\delta^{18}O$, $\alpha\_\delta^{2}H$) can be determined through laboratory experiments and Equations 8 and 11 (see Subsection 3.2 and 4.1). If we know the initial values within the air bag (q_0, $\delta^{18}O_0$, $\delta^{2}H_0$), the ambient values (q_e, $\delta^{18}O_e$, $\delta^{2}H_e$), and the storage time of the sampling bag, we are able to simulate the variations in humidity and isotopic ratios inside the air bag according to Equations 4 and 6. Similarly, if we know the storage time, the humidity and isotopic values at time t ($q(t)$, $\delta^{18}O_t$, $\delta^{2}H_t$) in the air bag, and the ambient values, we can deduce the initial values in the air bag at t = 0 by back-calculating.

https://doi.org/10.5194/amt-2024-151
Preprint. Discussion started: 4 November 2024

Atmospheric Measurement Techniques Discussions

3 Methods and data

3.1 Air bag isotope measurements

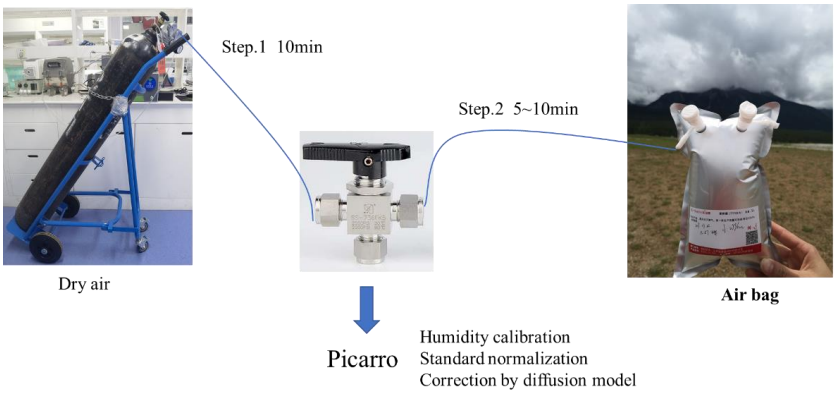

Figure 2 Setup for isotope measurements using air bags with a Picarro atmospheric water vapor isotope analyzer.

In this study, we used 0.5 L and 4L Teflon air bags produced by Dalian Hede Technologies Co., Ltd to collect and store vapor, and measured the vapor isotopes using a Picarro 2130i water isotope analyzer. Based on our testing and the airflow rate set for the Picarro analyzer, the 0.5 L and 4 L bags provided sufficient sample volume for approximately 25 minutes and 200 minutes of analysis, respectively.

Figure 2 illustrates the setup for measuring vapor isotopes in air bags. In this system, the air inlet of the Picarro isotope analyzer was connected to a three-way valve through Teflon or stainless steel tubing. The other two ports of the three-way valve were attached to the outlet valve of the air bag and a dry air cylinder, respectively. Sample storage and measurement were conducted in a temperature-regulated room to maintain constant temperature conditions for the air bags and tubing.

In the measurement procedure, we first activated the dry air cylinder and adjusted the pressure reducing valve to set the flow rate at 2 psi (pounds of force per square inch). We then opened the valve channel connecting the dry air cylinder to the three-way valve, allowing dry air to flow into the isotope analyzer and flush all air pathways for 10 minutes. Subsequently, we closed the dry air channel, opened the air bag outlet valve, and the corresponding valve channel on the three-way valve. This allowed water vapor in the air bags to be analyzed at a constant temperature in the Picarro analyzer, a process lasting between 5 and 10 minutes. Upon completion, we switched the valve to measure dry air. By repeatedly measuring isotope values for parallel samples, we can achieve greater accuracy in the water vapor measurements.

To correct the humidity-dependent isotope bias, we applied a calibration function by measuring vapor isotopes with gradient vapor concentrations set using a standard delivery module (SDM). We set a reference level of 20,000 ppm for vapor humidity in our analysis, considering the optimal accuracy of the Picarro analyzer at this specific humidity level

https://doi.org/10.5194/amt-2024-151
Preprint. Discussion started: 4 November 2024

Atmospheric Measurement Techniques Discussions

(JingfengLiu et al., 2014; Schmidt et al., 2010). All the measured vapor isotope data were normalized to the VSMOW-SLAP scale using two distinct laboratory waters with known isotopic values. Before conducting daily measurements, we adjusted the quantity of the injected liquid standard to align with the humidity of the external vapor measurements.

3.2 Laboratory permeability experiments

To evaluate the variations of the diffusion of water molecules between the interior and exterior of the air bags, we conducted the following experiments (Table 1), as detailed below:

Table 1 Summary of experiments: diffusion parameter quantification, model validation and differences in experimental methods. $\lambda\_{surface}$ denotes the diffusion coefficient of humidity at the surface, α_δ refers to the fractionation coefficient of isotopes, q_0 represents the initial vapor humidity in the air bags, and q_e corresponds to the environmental vapor humidity.

Experiment Number	Experimental purpose	Differences in experimental methods
No. 1	Quantification of $\lambda_{\_surface}$	Dry air in the air bags
No. 2	Quantification of α_δ	Water vapor with known isotopic compositions in the air bags under the condition $q_0 = q_e$
No. 3	Diffusion model validation	Water vapor with varying isotopic compositions and humidity levels in the air bags

3.2.1 Experiment No. 1: Quantification of $\lambda_{\_surface}$

To quantify the diffusion coefficient of humidity at the surface, $\lambda_{\_surface}$, using Equation 8, we filled the empty and clean air bags with dry air and measured humidity variations using a Picarro analyzer at intervals of 1 minute, 2, 4, 6, 8, and 10 hours following the measurement method described in Subsection 3.1. Measurements were conducted using 0.5L and 4L air bags, with repetitions on both identical and different air bags of the same dimensions (refer to the experiment times in Table 2 and results in Fig.3a). Results will be shown in Subsection 4.1.

3.2.2 Experiment No. 2: Quantification of α_δ

To investigate isotope variation patterns and improve measurement accuracy during storage in the air bag to quantify the isotopic fractionation coefficient, α, using Equation 11, initial values significantly different from ambient conditions were selected. Empty, clean air bags were filled with dry air, followed by the injection of a fixed amount of water with known isotopic values, ensuring that q_0 was approximately equal to q_e. To ensure $q_0 = q_e$, the environmental vapor concentration was first measured, followed by the calculation and experimental determination of the water volume to be injected into the air bag. Water vapor concentration and isotope variations within the air bags were then measured using a Picarro analyzer at intervals of 5 minutes, 2, 4, 6, 8, and 10 hours. Results will be shown in Subsection 4.1. To ensure data consistency and reliability, we repeated these measurements multiple times

https://doi.org/10.5194/amt-2024-151
Preprint. Discussion started: 4 November 2024


Atmospheric Measurement Techniques Discussions

using air bags of both the same and different sizes, including 0.5L and 4L bags. For the 0.5L air bags, a separate bag was prepared for each time interval, and water vapor concentration and isotopic compositions were measured once to ensure that the parameter M remained stable without being affected by repeated measurements. However, manual injection of water with known isotopic values introduced some variability, making it difficult to ensure identical initial conditions across all bags. To address this, we repeated the experiment with 4L air bags, measuring the same air bag at different time intervals, which ensured consistent initial conditions at t=0 but allowed M to change over time. When air bags differ only in size, the parameter λ associated with A varies, while the isotopic fractionation coefficient α is theoretically constant. Both approaches could contribute to uncertainties in the mismatches between the model and experimental results. Therefore, we incorporated the results from both the 0.5 L and 4 L experiments into our uncertainty estimation of these mismatches, as detailed in Subsections 3.2.3 and 3.4.2.

3.2.3 Experiment No. 3: Diffusion model validation

To validate the diffusion model under diverse conditions and evaluate its uncertainties, we repeated Experiment No. 2, but injected different amounts of water with known isotopic values to achieve a range of humidities from approximately 1/8 * q_e to q_e. Additionally, we used water with different isotopic values to replicate the experiment. To assess extended-duration variations, we also lengthened the time interval to 24 hours.

Once the parameters of the diffusion model have been obtained through Experiments No. 1 and 2, we can use this model to simulate the variations in water vapor humidity and isotope values inside the air bag over time for Experiments No. 2 and 3 (refer to Section 2). When simulating these experiments using the diffusion model, we used measurements taken after a 5-minute delay as the initial condition to ensure that it represented complete evaporation of the injected water. We then simulated the temporal variations in humidity and vapor isotopes within the air bag using a 5-minute time step. Results will be shown in Subsection 4.2.

3.3 Drone-mounted systems and field campaign

We designed and constructed a collection module for fixed-height sampling at predetermined altitudes, using air pumps and a rudder mounted on the drone, along with a control module linked to a remote operating system. However, as air pressure increases during the drone's descent after collection, the air bags may deflate, potentially causing leakage of the collected air samples. To address this, we installed a one-way valve that permits only air entry into the bag, thus preventing backflow. Additionally, the one-way valve helps prevent large droplets from entering the air bag during the collection process.

The sampling module was mounted on our specially designed high-altitude drones and deployed during a field campaign in the pristine forests region of Mountain Laojun, Lijiang, on the southeastern edge of the Tibetan Plateau and the northwestern of the Yunnan-Guizhou Plateau, China, throughout the period from June 25, 2020, to October 17, 2020.

By integrating high-altitude drone sampling with in-situ water vapor isotope measurements at the surface, we obtained vapor isotopic profiles up to an altitude of 11 km.

https://doi.org/10.5194/amt-2024-151
Preprint. Discussion started: 4 November 2024

Atmospheric Measurement Techniques Discussions

Unlike conventional methods, such as cryogenic vapor sampling, this approach requires much less sample volume and allows for in-situ measurements. Additionally, compared to large aircraft, airships, and balloon-based observations, this method is relatively low-cost and supports more flexible and long-term observations.

3.4 Application of diffusion model to vertical profiles

3.4.1 Estimating the air mass in the bag

For the vertical profile samples collected using drones, since λ (k*A/M) depends on M, and M acquired by the sampling bag varies due to different sampling altitudes with varying air pressure, λ consequently varies with altitude as well. However, it is difficult to experimentally estimate λ for different altitudes ($\lambda_{\_alt}$); instead, we estimated it from the variation of the collected M.

At higher altitudes, where the air pressure ($P_{\_alt}$) is lower than at the surface ($P_{\_surface}$), less air will be pumped into the air bag. To compensate for this effect, a longer sampling time was used at higher altitudes (Sampling $time_{\_alt}$) than at the surface (Sampling $time_{\_surface}$) (Fig.A1). Therefore,

$$M_{\_alt} = M_{\_surface} * \frac{P_{\_surface}}{P_{\_alt}} * \frac{\text{Sampling time}_{\_alt}}{\text{Sampling time}_{\_surface}} \quad (12)$$

where $M_{\_alt}$ is the air mass collected at a different altitude and $M_{\_surface}$ represents the air mass collected at the surface.

Therefore, the λ at a higher altitude ($\lambda_{\_alt}$) can be estimated as:

$$\lambda_{\_alt} = \lambda_{\_surface} * \frac{P_{\_surface}}{P_{\_alt}} * \frac{\text{Sampling time}_{\_alt}}{\text{Sampling time}_{\_surface}} \quad (13)$$

where $\lambda_{\_surface}$ is the λ quantified experimentally at the surface.

All sampling times were recorded during in-situ sampling. Given the variables $\lambda_{\_surface}$, Sampling $time_{\_alt}$, Sampling $time_{\_surface}$, $P_{\_surface}$ and $P_{\_alt}$, $\lambda_{\_alt}$ at different altitudes can be estimated using Eq. 13. The observed vertical profiles of vapor isotopes can then be corrected using the diffusion model described in Section 2 and quantified in Subsection 3.2. These estimates are subject to uncertainties, which will be discussed in the subsequent section 3.4.2.

3.4.2 The method of uncertainty estimation

Potential sources of error in the diffusion model correction process include estimates of $\lambda_{\_surface}$, $\alpha_{\_}\delta$, $\lambda_{\_alt}$, and from mismatches between model and experiments (Table 2).

For $\lambda_{\_surface}$, the uncertainty range was estimated through laboratory experiments by considering the minimum and maximum values obtained. The results are presented in Subsection 4.1.

For $\alpha_{\_}\delta$, the average values of λ and λ/α were estimated from several experiments, and then α can be calculated. The results are presented in Subsection 4.1. In Subsection 4.2, we observed that the values simulated by the model closely track the experimental results, thereby validating the accuracy of our parameter selection. For the uncertainty range of $\alpha_{\_}\delta$, it is also

https://doi.org/10.5194/amt-2024-151
Preprint. Discussion started: 4 November 2024

Atmospheric Measurement Techniques Discussions

essential to first validate the parameters derived from the experiments. As highlighted in Subection 3.2.2, estimating λ/α (and subsequently calculating α) requires results from cases where q_0 equals q_e. However, in these numerous experiments, it cannot be guaranteed that all q_0 exactly equal q_e, and q_e can exhibit temporal variations, leading to non-systematic discrepancies between the model and experimental data. Consequently, for analyzing the contribution of α to uncertainties, only α values derived from experiments where the model closely matched the majority of experimental results were considered. Selection criteria for these experiments included minimal deviation between q_0 and q_e, minimal deviation between experimental data and simulations, and stable q_e values, ensuring the reliability of the chosen α values.

Regarding the sampling time, we note that using the same air pump to extract air under varying atmospheric pressures for an identical duration may result in different air mass, M. To compensate for this potential variability, we incorporated a larger margin of error for the recorded sampling time. Consequently, when calculating $\lambda_{\_alt}$ using Equation 13, we considered a relative uncertainty of ± ¼ of the recorded sampling time.

To address the mismatch between the model and the experiment, we gathered all experimental data and conducted simulations using the diffusion model. We simulated variations in humidity and isotopic composition based on the initial values within the air bag, ambient conditions, and the storage time of the sampling bag, as described in Subsection 2.2. We then calculated the differences between the simulations and the experimental data for each corresponding storage time. Finally, we computed the average of all these differences for each parameter separately. The results are presented in Subsection 4.2.

To evaluate the total error, we computed the maximum discrepancy between all calibration results, which used the uncertainty ranges of the first three potential sources mentioned above, and the corrected data employed. To this value, we added the fourth error source, which is the mismatch observed between the model and the experiments. The final uncertainties present in Subsections 4.3 and 4.5 represent the maximum error derived from all four error sources.

Table 2 Uncertainty sources and estimation methods

Uncertainty sources	Number of experiments	Estimation method	Used value (min~max for error estimation)
$\lambda_{\_surface}$	7; 6	Obtained from lab experiments (max & min)	For 0.5L air bags: 0.031(0.0291~0.0317); For 4L air bags: 0.0255(0.0250~0.0259)
α_δ	4	Obtained from lab experiments	α_δ^{18}O is 1.0241, α_δ^{2}H is 1.0451 (α_δ^{18}O is 1.0254, α_δ^{2}H is 1.0506 and α_δ^{18}O is 1.0264, α_δ^{2}H is 1.0380)
Sampling $time_{\_alt}$	-	Recorded sampling time	± ¼
Mismatches between model and experiments	87	Average of all difference between experimental data and simulations	0.5 ‰ for δ^{18}O, 4.1 ‰ for δ^{2}H, 2.9 ‰ for d-excess

https://doi.org/10.5194/amt-2024-151
Preprint. Discussion started: 4 November 2024

Atmospheric Measurement Techniques Discussions

3.5 Satellite isotope data IASI

Of the available instruments, the Infrared Atmospheric Sounding Interferometer (IASI) offers the best spatiotemporal coverage for δ^2H retrieval (Lacour et al., 2012; Lacour et al., 2018). It has a horizontal footprint of approximately 12 km at nadir (directly below the satellite), increasing with the angle of observation. This configuration ensures nearly global coverage twice daily.

In this study, we compared our observed vapor δ^2H profiles up to the upper troposphere with satellite observations. Due to the intermittent availability of IASI data at any given location, we limited our comparison of observational results across various altitudes at our study site to days when IASI data were available. Satellite measurements, particularly for water vapor isotopes, typically have limited vertical resolution. The IASI satellite instrument provides water vapor isotope data at three altitude levels: 1-3 km in the lower troposphere, 4-7 km in the mid-troposphere, and 8-12 km in the upper troposphere. Given that our study started at an altitude of 3856 m, we used the retrieved δ^2H data for the 4–7 km and 8–12 km levels. However, these measurements represent a vertical average over layers determined by the averaging kernels (Rodgers and Connor, 2003; Worden et al., 2006). While using averaging kernels to smooth the observed profile could facilitate a more quantitative analysis, we simply averaged the observations for the corresponding altitudes. Consequently, the comparison remains mainly qualitative.

4 Results

4.1 Parameter estimates

The $\lambda_{\_surface}$ was determined through laboratory Experiment No. 1. Based on Equation 8, the parameter $\lambda\_surface$ was estimated to be 0.0312 (uncertainty range: 0.0291 to 0.0317) for the 0.5 L air bags and 0.0255 (uncertainty range: 0.0250 to 0.0259) for the 4 L air bags (Fig. 3a, Table 2).

The isotopic fractionation coefficients, α, were determined through laboratory Experiment No. 2. From the averaged results of these measurements, using Equation 11, the diffusion coefficient of isotopic composition, expressed as λ/α, was estimated to be 0.0249 for $\delta^{18}O$ and 0.0244 for δ^2H (Fig. 3b and c). Consequently, $\alpha\_\delta^{18}O$ was estimated to be 1.0241 (0.0255/0.0249), and α_δ^2H was estimated to be 1.0451 (0.0255/0.0244) (Fig. 3b and d). Two additional sets of fractionation coefficients, α, were obtained: $\alpha\_\delta^{18}O = 1.0254$, $\alpha\_\delta^2H = 1.0506$, and $\alpha\_\delta^{18}O = 1.0264$, $\alpha\_\delta^2H = 1.0380$ (Table 2).

These parameters determined were influenced by factors such as the type and material composition of the air bags and ambient temperature. The acquired parameters specifically pertained to the Teflon air bags used in the aforementioned tests, conducted at an ambient temperature of 16°C. We observed some differences between batches of air bags from the same manufacturer, which are worth noting. The primary objective of this study was to establish a methodology.

https://doi.org/10.5194/amt-2024-151
Preprint. Discussion started: 4 November 2024

Atmospheric Measurement Techniques Discussions

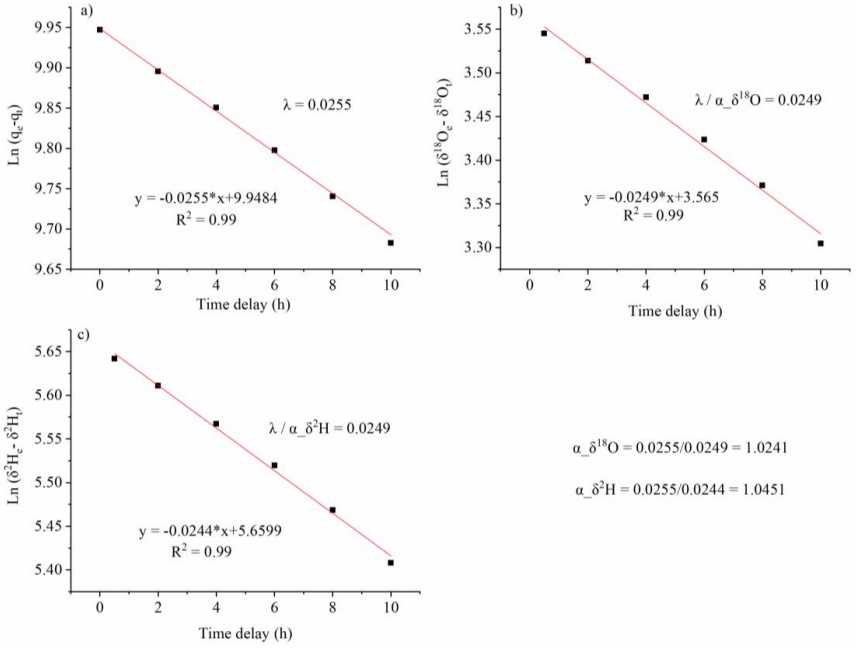

381

Figure 3 Determination of 3 parameters of the diffusion model : $\lambda\_{surface}$ (a), $\alpha\_\delta^{18}O$ (b), and $\alpha\_\delta^{2}H$ (c).

https://doi.org/10.5194/amt-2024-151
Preprint. Discussion started: 4 November 2024

Atmospheric Measurement Techniques Discussions

4.2 Diffusion model validation

4.2.1 General case

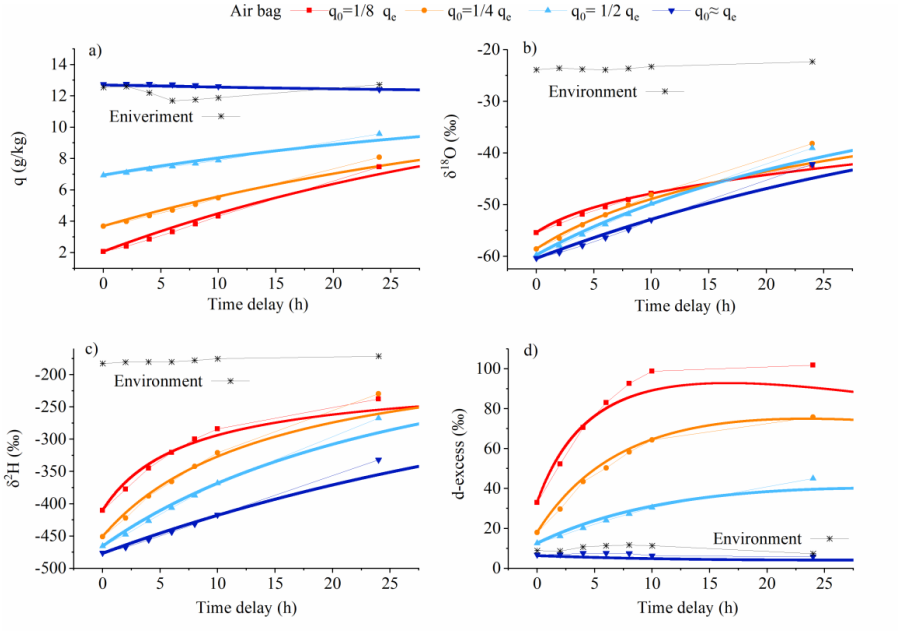

*Figure 4: Comparison of the variation within the air bag over time in laboratory permeability experiments (markers) and diffusion model simulations (lines) across a range of initial humidities at t = 0 (q_0), ranging from approximately 1/8 * q_e to q_e (q_e denotes the environmental humidity), under the condition that the water vapor isotopic composition in the air bag significantly differs from ambient values : a) humidity; b) $\delta^{18}O$; c) $\delta^{2}H$, d) d-excess.*

To validate the model, we used Experiment No.3 described in Subsection 3.2. The simulations from our diffusion model are in close agreement with our experimental observations, with only minor deviations (Fig.4). Shorter storage times produce fewer deviations. When the humidity inside the air bag is lower than the ambient level, vapor from the environment enters the air bag, resulting in a gradual increase in humidity (Fig. 4a). Meanwhile, because the water vapor isotopic composition in the air bag is significantly lower than the ambient values, $\delta^{18}O$ and $\delta^{2}H$ in the air bag gradually increase and toward ambient values as ambient moisture enters the bags over time (Fig. 4b and c). In contrast, the d-excess values increase as the time delay progresses due to kinetic fractionation during moisture diffusion into the air bag (Fig. 4d), as detailed in the following Subsection 4.2.2.

https://doi.org/10.5194/amt-2024-151
Preprint. Discussion started: 4 November 2024

395 **4.2.2 Particular cases**

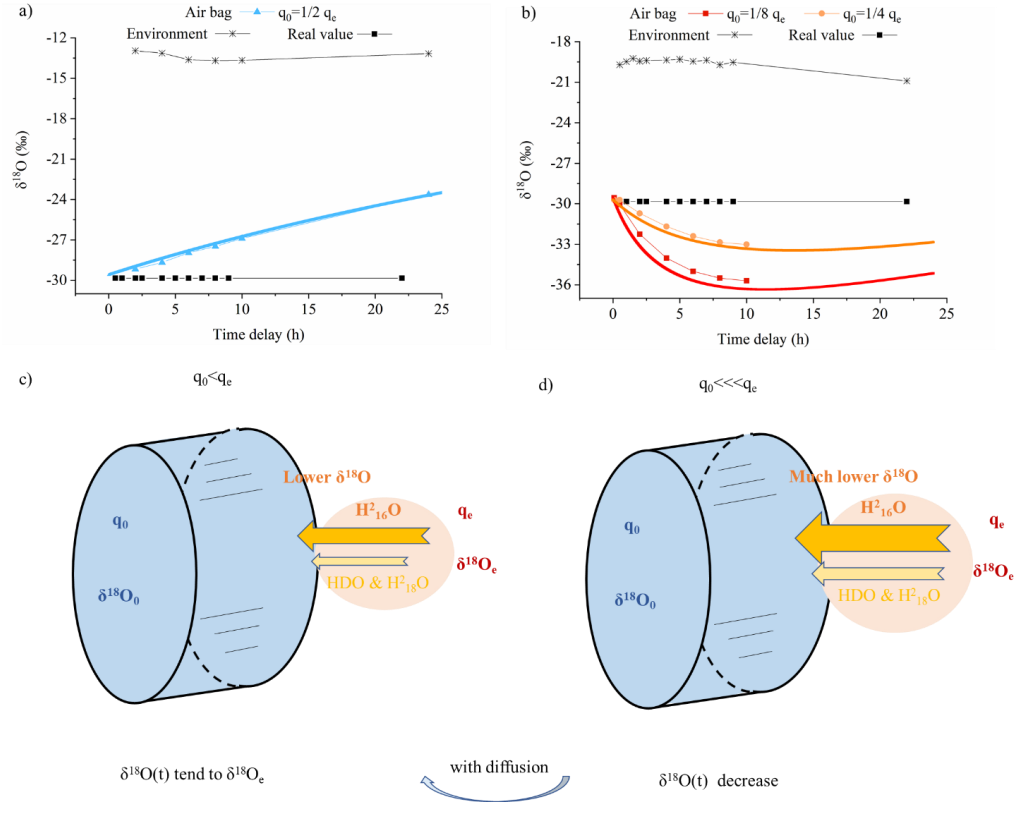

396

Figure 5 (a, b) (a-b) Variations of $\delta^{18}O$ under different conditions: (a) the differences between internal ($\delta^{18}O_0$) and external ($\delta^{18}O_e$) $\delta^{18}O$ values as well as between internal (q_0) and external (q_e) humidity are not significant; (b) the difference between $\delta^{18}O_0$ and $\delta^{18}O_e$ is less pronounced, and q_0 is significantly lower than q_e. (c,d) Corresponding schematic illustrations of the underlying mechanisms for (a) and (b). $\delta^{18}O$ (t) is the variation of $\delta^{18}O$ within the air bag over time.

397 Due to isotopic kinetic fractionation, $H_2{}^{16}O$ molecules preferentially diffuse into the air
398 bag compared to HDO and $H_2{}^{18}O$, resulting in a vapor flux with lower $\delta^{18}O$ (Fig. 2). Moreover,
399 variations within the air bag are driven by differences in water vapor content and isotopic ratios
400 between its interior and exterior, as described in the diffusion model in Section 2. As shown in
401 the first scenario in Figure 4b and c: when the internal $\delta^{18}O$ and δ^2H values are significantly
402 below the ambient values, the δ-values of the diffusing vapor, although lower than ambient,
403 still exceeds the initial internal δ-values, leading to a gradual increase towards the ambient
404 values; diffusion simply equilibrates the isotopic composition in the bag and the environment.
405 Similarly, in the second scenario in Figure 5a and c, when the disparity between internal and
406 external $\delta^{18}O$ and δ^2H values is not very substantial, and humidity differences are also minimal,

https://doi.org/10.5194/amt-2024-151
Preprint. Discussion started: 4 November 2024

Atmospheric Measurement Techniques Discussions

the weaker diffusive gradient produces less net kinetic fractionation. This results in a small amount of vapor with lower $\delta^{18}O$ and $\delta^{2}H$ values entering preferentially, but not falling below internal initial values, thereby driving a progressive increase in the internal values towards ambient values as in the first scenario. In contrast, in the third scenario in Figure 5b and d, with the same initial contrast between internal and ambient δ-values, that is, the disparity between internal and external $\delta^{18}O$ and $\delta^{2}H$ values is less pronounced, but q_0 is much lower than q_e, there is a stronger net flux into the bag, and this flux fractionates more rapidly; much more vapor with significantly lower $\delta^{18}O$ and $\delta^{2}H$ values than the ambient moisture (and lower values than the initial internal vapor) enters the air bags and dominates their isotopic composition, thereby reducing the internal δ-values. As diffusion progresses, the difference in humidity and isotopic composition between the inside and outside of the air bag decreases, causing the third scenario to evolve into the second scenario. The smaller the difference in humidity and isotopic composition between the inside and outside of the air bag, the slower and smaller the isotopic change in the vapor within the air bags (Fig. 5 and Fig. 6).

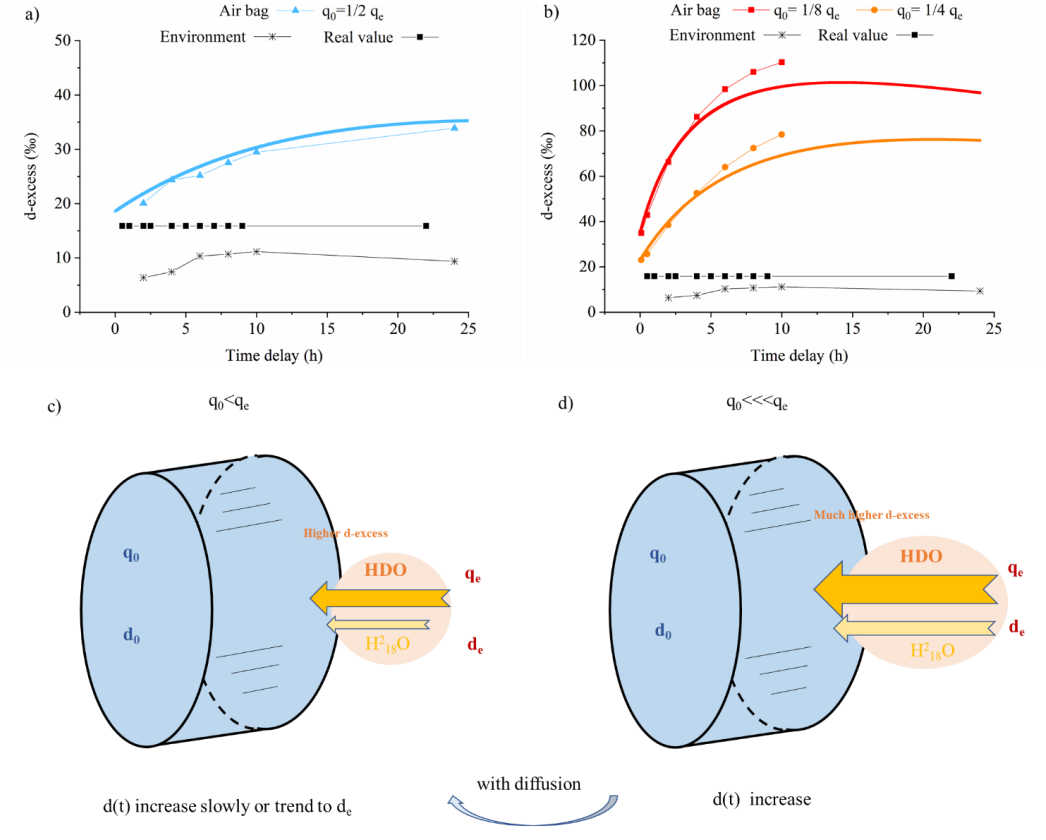

Figure 6 (a-b) Evolution of d-excess in cases: (a) the difference between the humidity inside (q_0) and outside (q_e) the air bag is not significant; (b) q_0 is significantly lower than q_e. (c-d) Corresponding schematic illustrations of the underlying mechanisms for (a) and (b). d_0 indicates the initial d-excess value at t = 0, d_e represents the d-excess in the environment. d(t) denotes the variation of d-excess within the air bag over time.

https://doi.org/10.5194/amt-2024-151
Preprint. Discussion started: 4 November 2024

Atmospheric Measurement Techniques Discussions

In addition, because HDO and $H_2{}^{18}O$ diffuse at similar rates the magnitude of the kinetic fractionation for D and ^{18}O is similar. However, since d-excess reflects deviations relative to the 8:1 fractionation ratio typical of equilibrium processes, the tendency is for kinetic fractionation during diffusion to contribute vapor with high d-excess and cause an increase in d-excess during air bag storage as water vapor is added to the bag (Fig. 6a and c). When the humidity difference between the inside and outside of the air bag increases, the d-excess of the incoming vapor flux increases as a result of more intensive kinetic fractionation. This leads to a faster increase in the vapor d-excess value inside the air bag (Fig. 6b and d).

In all scenarios, regardless of the differences in water vapor humidity and isotopic compositions inside and outside the air bag, the diffusion model simulations closely match the experimental observations (Figs.5 and 6). Using the method described in Subsection 3.4.2, the average difference between all simulations and experimental data for each parameter represented the model-experiment mismatch: 0.5 ‰ for $\delta^{18}O$, 4.1 ‰ for $\delta^{2}H$, and 2.9 ‰ for d-excess.

4.3 **Raw and corrected vertical profiles**

Here, we present a summary of drone-based observations from the field campaign at Mount Laojun, Lijiang, on the southeastern edge of the Tibetan Plateau and the northwestern of the Yunnan-Guizhou Plateau, China, conducted between June 25, 2020, and October 17, 2020. In this dataset, acquired from the drones observations and subsequently corrected using the diffusion modeling, data points with d-excess values less than 1‰ were omitted, as these values are unrealistic and likely result from overcorrection of the δ-values. This resulted in the exclusion of 6 out of 1039 samples.

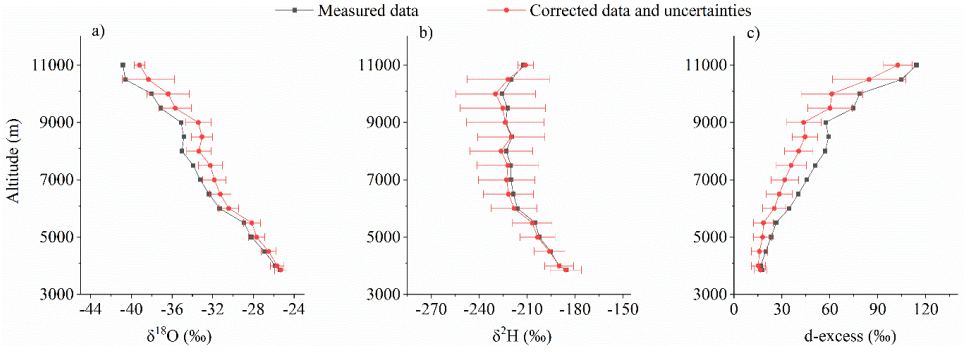

Figure 7 Comparison of vertical profiles for the mean values of all raw measurements and corrected data from June to October, and associated uncertainties for $\delta^{18}O$ (a), $\delta^{2}H$ (b) and d-excess (c).

As altitude increases, vapor $\delta^{18}O$ and $\delta^{2}H$ values decrease due to condensation and precipitation processes that occur as air masses ascend, which preferentially remove heavier isotopes following Rayleigh distillation (Dansgaard, 1964). Meanwhile, the d-excess value rises. This pattern aligns with previous observations in the lower troposphere (He and Smith, 1999; Salmon et al., 2019) and simulations of complete vertical profiles (Bony et al., 2008).

https://doi.org/10.5194/amt-2024-151
Preprint. Discussion started: 4 November 2024

Atmospheric Measurement Techniques Discussions

In our observations, the variation in $\delta^{18}O$ across the vertical profile from ground level at 3856 meters to 11 km is approximately 10-15‰. However, as altitude increases, the air becomes progressively drier, leading to a greater disparity in humidity between the air collected in the air bag and the surface storage environment. This aligns with the third scenarios in Subsection 4.2.2 (Figs. 5b, 5d, and 6b, 6d). The strong kinetic fractionation driven by the diffusion of air into the air bag results in a reduction of the water vapor $\delta^{18}O$ within the bag. After applying model corrections, the initial vapor $\delta^{18}O$ inside the air bag were slightly increased. As described in Subsection 4.2, during storage in the air bag, vapor flux with higher d-excess increases the d-excess in the air bags. As a compensation, the diffusion model applies corrections, resulting in a reduced d-excess value after correction (Fig. 7c and 10).

4.4 Uncertainty estimates

According to the method of uncertainty estimation elaborated in Subsection 3.4.2, we determined the ranges for four error sources to evaluate uncertainty (Table 2).

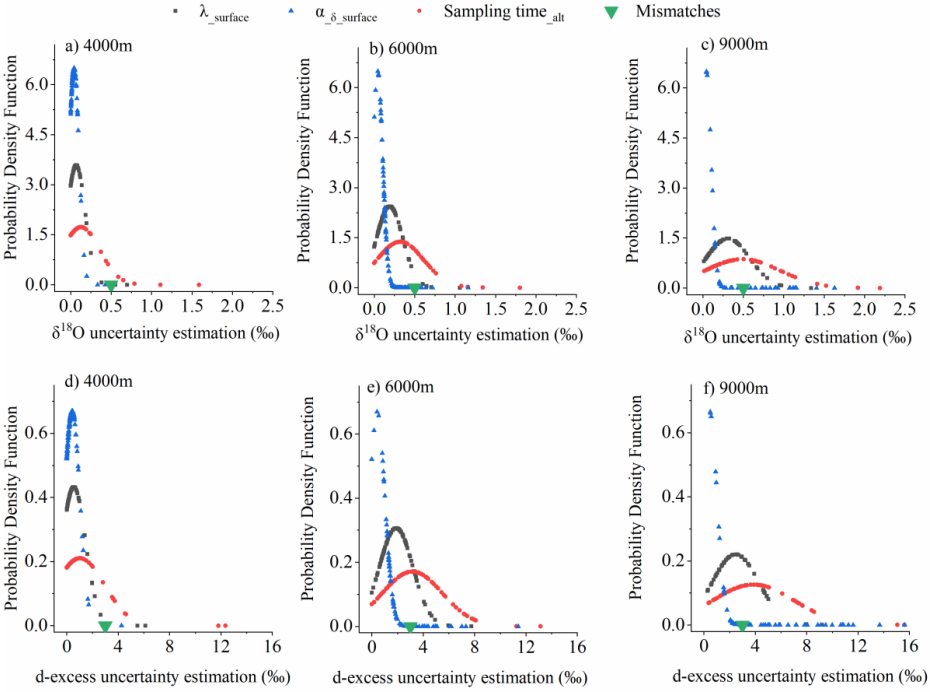

Figure 8: Contributions of different sources of uncertainty for $\delta^{18}O$ (a, b, c for 4000m, 6000m, 9000m, respectively) and d-excess (d, e, f for 4000m, 6000m, 9000m, respectively). The green triangle shows the average mismatch between the model and experimental results.

We analyzed the contributions of uncertainty sources to vertical vapor $\delta^{18}O$ and d-excess measurements at different altitudes using probability density function plots (Fig. 8). The mismatch between the model and the experiment (green marker), calculated using the method

https://doi.org/10.5194/amt-2024-151
Preprint. Discussion started: 4 November 2024

Atmospheric Measurement Techniques Discussions

described in Subsection 3.4.2, is assumed to remain constant across all altitudes. The other three error sources manifest as unimodal normal distributions at various altitudes for both $\delta^{18}O$ and d-excess. Errors due to uncertainties in Sampling time$_{alt}$ are the main source, exhibiting the largest spread (Fig. 8) and increasing with altitude (Fig. 9). Errors derived from $\lambda_{surface}$ and α_δ values also increase with altitude (Figs. 8 and 9). This pattern emerges because, estimating λ_{alt} correlated with M based on $\lambda_{surface}$, with M at high altitude derived from the Sampling time$_{alt}$ using Equation 13. This approach can introduce more significant errors at higher altitudes. As altitude increases, the humidity and isotopic disparity between the air captured in the air bag and lower-altitude ambient conditions widens, requiring more intensive corrections. Consequently, both the uncertainty (Figs. 8 and 9) and the magnitude of the diffusion correction (Fig. 7) increase with altitude. Overall, the total error remains within 1‰ for $\delta^{18}O$ and 8‰ for d-excess across 98% of the data.

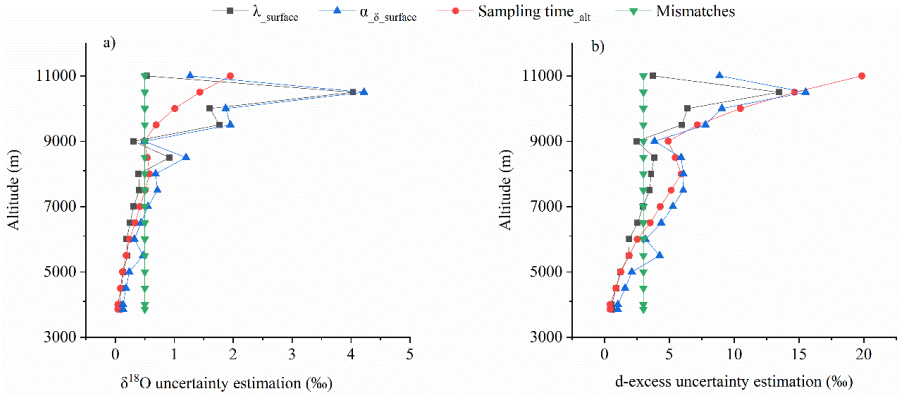

Figure 9 Mean uncertainty of $\delta^{18}O$ (a) and d-excess (b) with altitude for different sources.

On the contrary, errors pertaining to $\lambda_{surface}$ and α_δ diminish at altitudes exceeding 10,500 meters. This phenomenon may be attributed to our sampling methodology. Although we collected air samples in sequence from low to high altitudes, these samples were measured in reverse order, from high to low altitudes. Consequently, samples taken from the highest altitudes had the shortest storage durations, typically ranging from 10 minutes to two hours. Additionally, we extended the sampling times with increasing altitude (Fig. A1). These extended sampling periods and reduced storage durations help to partially offset the amplified disparities observed between the raw and corrected profiles at higher altitudes. During the drone's descent, which lasted around 10 minutes, the external conditions impacting the air bags were not the ground-level environmental values used in the model but rather those of the vertical profile. However, the humidity at higher altitudes is lower than at ground level, and the isotopic values are closer to those inside the airbag. Consequently, its impact on the airbag's internal conditions is less significant than suggested by using ground-level environmental values. Therefore, the overestimated error in our model accounted for these potential discrepancies.

https://doi.org/10.5194/amt-2024-151
Preprint. Discussion started: 4 November 2024

Atmospheric Measurement Techniques Discussions

4.5 Comparison with Picarro measurements and satellite data

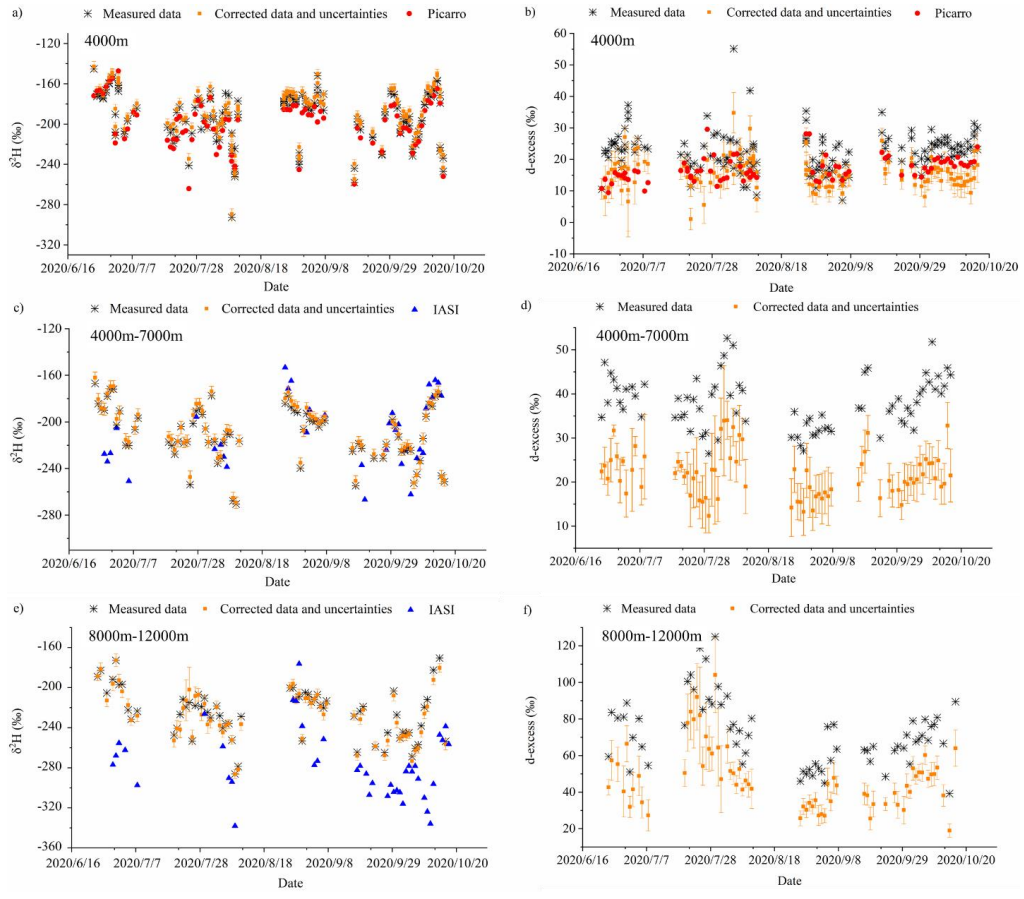

Figure 10 Time series comparison for $\delta^{18}O$ (a, c, e) and d-excess (b, d, f):

(a, b) Raw and corrected (with uncertainties) altitude-averaged air bag measurements from 3856 m to 4000 m, compared with direct Picarro observations at 3856 m.

(c, d) Raw and corrected (with uncertainties) altitude-averaged air bag measurements from 4000 m to 7000 m, compared with satellite data (IASI).

(e, f) Raw and corrected (with uncertainties) altitude-averaged air bag measurements from 8000 m to 12000 m, compared with satellite data (IASI).

The left panel of Figure 10 (Fig. a, c, and e) shows the comparison of raw and corrected water vapor $\delta^{18}O$ measurements at different altitudes with direct Picarro observations or IASI satellite data at corresponding altitudes. There is notable agreement between the raw measurements and corrected $\delta^{18}O$ for altitudes 3856-4000m and the water vapor $\delta^{18}O$ observed directly by Picarro at ground level (3856m) (Fig.10a). To compare corrected measurements with independent observations at higher altitudes, we refer to the IASI satellite dataset. We

https://doi.org/10.5194/amt-2024-151
Preprint. Discussion started: 4 November 2024


Atmospheric Measurement Techniques Discussions

acknowledge that this comparison is complicated by differences in measurement footprints (both horizontal and vertical) and spatio-temporal sampling disparities (Shi et al., 2020). Therefore, this comparison remains qualitative. For most intervals, IASI satellite data closely matches raw and corrected $\delta^{18}O$ measurements for altitudes 4000–7000m. In the 8000–12000m range, IASI data is lower than $\delta^{18}O$ observations during certain periods, particularly June and September 2020. While the IASI data closely matches the observed $\delta^{18}O$ values for all other periods in the 4000–7000 meter range, it is also lower in June 2020. A more quantitative analysis could be facilitated if an averaging kernel is used to smooth the observed profiles (Herman et al., 2014). All comparisons reflect consistent temporal variations.

The right panel of Figure 10 (Fig. b, d, and f) shows the comparison of raw and corrected vapor d-excess measurements. In the 4000m observations (Fig. b), raw d-excess values in air bags were higher than corrected values due to kinetic fractionation during diffusion. After correction, d-excess values decrease and are similar to surface direct Picarro observations at 3856 m. For the 4000–7000m and 8000–12000m observations, no d-excess dataset is available for comparison (Fig. 10d and f). As previously noted, raw d-excess values are higher than corrected data due to kinetic fractionation. After correction, d-excess decreases. For the 8000–12000 m observations, the correction magnitude is smaller than at lower altitudes due to the shorter storage time of the air bags.

5 Conclusion

High spatial and temporal resolution water vapor isotope data are critical for understanding various hydrologic cycle processes. However, observations of vertical water vapor isotope profiles are scarce, particularly in the upper troposphere. Satellite-derived vapor isotope data are available only at limited vertical and temporal resolutions. Acquiring high-resolution water vapor isotope data, especially under conditions where direct measurements are difficult, has been a significant challenge for the water isotopes research community. This study demonstrates the potential of a drone-based air bag sampling method to overcome this challenge and offers solutions for evaluating air bag suitability and addressing air bag permeability.

While air bags offer the advantage of sample collection, their inherent permeability can affect the sealing integrity of the samples, leading to potential contamination. The permeability of airbag materials varies, with some exhibiting lower levels. We recommend prioritizing the use of glass containers and air bags with the lowest permeability for collecting water vapor using portable devices. Additionally, it is essential to conduct the permeability experiments described in this article before any experimental undertaking. This involves storing water vapor with known isotopic values in the portable collection device for an extended period and then re-measuring these values to assess or determine the device's permeability parameters.

To further address the permeability challenge, we developed a mathematical model to evaluate and correct for diffusion and isotopic fractionation, ensuring the reliability of vapor isotope measurements using air bags. Calibrated with parameters from laboratory experiments, our correction model reconstructs the initial isotopic composition of sampled vapor by using data from both the air bag and the surrounding environment, offers a practical solution to the

https://doi.org/10.5194/amt-2024-151
Preprint. Discussion started: 4 November 2024

Atmospheric Measurement Techniques Discussions

prevalent permeability challenges. This model was rigorously validated against observational experiments conducted under varying conditions. We also applied this model to drone-collected samples at various pressures. By estimating uncertainty and comparing corrected data with satellite observations, we validated the reliability and applicability of drone-based water vapor isotope measurements.

Our drone-based sampling system, combined with the diffusion model, effectively addresses the limitations of traditional laser spectroscopy methods, meeting the need for lightweight equipment and providing a more economical, efficient, and flexible solution for high-altitude water vapor measurements compared to traditional methods involving large aircraft, airships, and balloons. This approach enables us to exploit the benefits of drone-based air bag sampling while effectively mitigating its potential limitations. This strategy significantly broadens its potential applications across various environments, thereby enhancing the range and richness of data that can be gathered for water vapor isotope research.

Appendix A

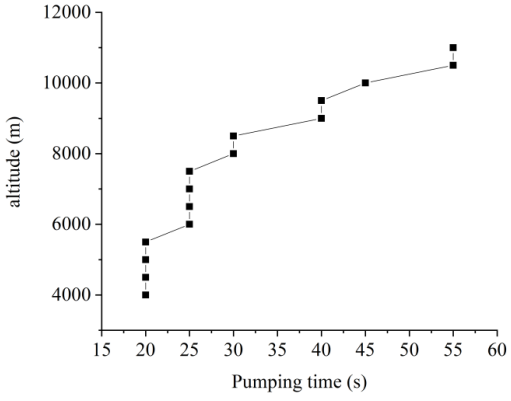

Figure A1 Sampling duration variation with altitude.

Code availability

The diffusion modeling code, which simulates the evolution of water vapor isotopes in the airbag and corrects them to their initial values, is available at:

https://github.com/DishiWANG0608/Correcting-for-water-vapor-diffusion.git

https://doi.org/10.5194/amt-2024-151
Preprint. Discussion started: 4 November 2024


Atmospheric Measurement Techniques Discussions

Data availability

Data are available from the authors on request.

Video supplement

A video showcasing our field campaign on drone-derived water vapor isotope sampling up to the upper troposphere (11 km) during convective activity, including the workflow for airbag water vapor isotope sampling, is currently available upon request and will be publicly accessible in the near future. Please contact the corresponding author for access (di.wang@lmd.ipsl.fr).

Author contributions

D.W., C.R., and L.T. designed the research, established the subjects of the methodology, and performed the analysis; D.W. and D.Y. conducted the observations; J.B., S.T., H.P. and L.L. contributed to the establishment of methodologies, data calibration, and analysis; Y.S. provided assistance with the computing; All authors contributed to the discussion of the results and the final article; D.W. drafted the manuscript with contributions from all co-authors.

Competing interests

The contact author has declared that none of the authors has any competing interests.

Acknowledgments

The authors gratefully acknowledge the Infrared Atmospheric Sounding Interferometer (IASI) for providing spatiotemporal coverage of δ^2H retrieval. We thank Jiaping Xu, Mingjian Chen, Le Chan, and Yao Yao for their irreplaceable help in the development of the drones. We are grateful to the management of 99 Dragon, Mountain Laojun in Lijiang for facilitating the field experiments. We thank Pengbin Liang and Jiangrong Tai for partially participating in the field observations. We acknowledge Hans Christian Steen-Larsen and Harald Sodemann for their discussions on the correction method. We acknowledge the use of OpenAI's ChatGPT to assist in refining the language. This work was supported by the National Natural Science Foundation of China (U2202208), the Strategic Priority Research Program of the Chinese Academy of Sciences (XDB40000000), and the Science and Technology Department of Yunnan Province (202201BF070001-021). Di Wang acknowledges support from Chinese Scholarship Council and the Postdoctoral Fellowship Program of CPSF under Grant Number GZC20241440. Siteng Fan acknowledges support from the Marie Skłodowska-Curie Actions

https://doi.org/10.5194/amt-2024-151
Preprint. Discussion started: 4 November 2024

of European Research Executive Agency (101064814) and the High Level Special Fund of Southern University of Science and Technology (G03050K001).

References

Ayliffe, L., Cerling, T., Robinson, T., West, A., Sponheimer, M., Passey, B., Hammer, J., Roeder, B., Dearing, M., and Ehleringer, J.: Turnover of carbon isotopes in tail hair and breath CO 2 of horses fed an isotopically varied diet, Oecologia, 139, 11-22, 2004.

Bony, S., Risi, C., and Vimeux, F.: Influence of convective processes on the isotopic composition (δ18O and δD) of precipitation and water vapor in the tropics: 1. Radiative-convective equilibrium and Tropical Ocean–Global Atmosphere–Coupled Ocean-Atmosphere Response Experiment (TOGA-COARE) simulations, Journal of Geophysical Research: Atmospheres, 113, 2008.

Bowen, G. J., Cai, Z., Fiorella, R. P., and Putman, A. L.: Isotopes in the Water Cycle: Regional-to Global-Scale Patterns and Applications, Annual Review of Earth and Planetary Sciences, 47, 2019.

Brienen, R. J., Schöngart, J., and Zuidema, P. A.: Tree rings in the tropics: insights into the ecology and climate sensitivity of tropical trees, Tropical tree physiology: adaptations and responses in a changing environment, 2016. 439-461, 2016.

Cerling, T. E., Wittemyer, G., Rasmussen, H. B., Vollrath, F., Cerling, C. E., Robinson, T. J., and Douglas-Hamilton, I.: Stable isotopes in elephant hair document migration patterns and diet changes, Proceedings of the National Academy of Sciences, 103, 371-373, 2006.

Dansgaard, W.: Stable isotopes in precipitation, Tellus, 16, 436-468, 1964.

Galewsky, J., Steen-Larsen, H. C., Field, R. D., Worden, J., Risi, C., and Schneider, M.: Stable isotopes in atmospheric water vapor and applications to the hydrologic cycle, Reviews of Geophysics, 54, 2016.

Gat, J. R.: Oxygen and hydrogen isotopes in the hydrologic cycle, Annual Review of Earth and Planetary Sciences, 24, 225-262, 1996.

Ghosh, P. and Brand, W. A.: Stable isotope ratio mass spectrometry in global climate change research, International Journal of Mass Spectrometry, 228, 1-33, 2003.

Gralher, B., Herbstritt, B., and Weiler, M.: Unresolved aspects of the direct vapor equilibration method for stable isotope analysis (δ 18 O, δ 2 H) of matrix-bound water: unifying protocols through empirical and mathematical scrutiny, Hydrology and Earth System Sciences, 25, 5219-5235, 2021.

Grootes, P. M. and Stuiver, M.: Oxygen 18/16 variability in Greenland snow and ice with 10(-3)- to 10(5)-year time resolution, Journal of Geophysical Research-Oceans, 102, 26455-26470, 1997.

He, H. and Smith, R. B.: Stable isotope composition of water vapor in the atmospheric boundary layer above the forests of New England, Journal of Geophysical Research Atmospheres, 104, 11657-11673, 1999.

Hendry, M., Schmeling, E., Wassenaar, L., Barbour, S., and Pratt, D.: Determining the stable isotope composition of pore water from saturated and unsaturated zone core: improvements to the direct vapour equilibration laser spectrometry method, Hydrology and Earth System Sciences, 19, 4427-4440, 2015.

Herbstritt, B., Gralher, B., Seeger, S., Rinderer, M., and Weiler, M.: Discrete in situ vapor sampling for subsequent lab-based water stable isotope analysis, Hydrology and Earth System Sciences, 27, 3701-3718, 2023.

Herman, R., Cherry, J., Young, J., Welker, J., Noone, D., Kulawik, S., and Worden, J.: Aircraft

https://doi.org/10.5194/amt-2024-151
Preprint. Discussion started: 4 November 2024

Atmospheric Measurement Techniques Discussions

validation of Aura Tropospheric Emission Spectrometer retrievals of HDO/H 2 O, Atmospheric Measurement Techniques, 7, 3127-3138, 2014.

Hodges, J. T. and Lisak, D.: Frequency-stabilized cavity ring-down spectrometer for high-sensitivity measurements of water vapor concentration, Applied Physics B, 85, 375-382, 2006.

Jiménez-Rodríguez, C. D., Coenders-Gerrits, M., Bogaard, T., Vatiero, E., and Savenije, H.: comparison of water vapor sampling techniques for stable isotope analysis, Hydrology and Earth System Sciences Discussions, 2019. 1-15, 2019.

Johnson, L., Sharp, Z., Galewsky, J., Strong, M., Van Pelt, A., Dong, F., and Noone, D.: Hydrogen isotope correction for laser instrument measurement bias at low water vapor concentration using conventional isotope analyses: application to measurements from Mauna Loa Observatory, Hawaii, Rapid Communications in Mass Spectrometry, 25, 608-616, 2011.

Lacour, J.-L., Risi, C., Clarisse, L., Bony, S., Hurtmans, D., Clerbaux, C., and Coheur, P.-F.: Mid-tropospheric δD observations from IASI/MetOp at high spatial and temporal resolution, Atmospheric chemistry and physics, 12, 10817-10832, 2012.

Lacour, J.-L., Risi, C., Worden, J., Clerbaux, C., and Coheur, P.-F.: Importance of depth and intensity of convection on the isotopic composition of water vapor as seen from IASI and TES δD observations, Earth and planetary science letters, 481, 387-394, 2018.

Michener, R. and Lajtha, K.: Stable isotopes in ecology and environmental science, John Wiley & Sons, 2008.

Millar, C., Pratt, D., Schneider, D. J., and McDonnell, J. J.: A comparison of extraction systems for plant water stable isotope analysis, Rapid Communications in Mass Spectrometry, 32, 1031-1044, 2018.

Muccio, Z. and Jackson, G. P.: Isotope ratio mass spectrometry, Analyst, 134, 213-222, 2009.

Rodgers, C. D. and Connor, B. J.: Intercomparison of remote sounding instruments, Journal of Geophysical Research: Atmospheres, 108, 2003.

Rozmiarek, K. S., Vaughn, B. H., Jones, T. R., Morris, V., Skorski, W. B., Hughes, A. G., Elston, J., Wahl, S., Faber, A.-K., and Steen-Larsen, H. C.: An unmanned aerial vehicle sampling platform for atmospheric water vapor isotopes in polar environments, Atmospheric Measurement Techniques, 14, 7045-7067, 2021.

Salmon, O. E., Welp, L. R., Baldwin, M. E., Hajny, K. D., Stirm, B. H., and Shepson, P. B.: Vertical profile observations of water vapor deuterium excess in the lower troposphere, Atmospheric Chemistry and Physics, 19, 11525-11543, 2019.

Shi, X., Risi, C., Pu, T., Lacour, J. l., Kong, Y., Wang, K., He, Y., and Xia, D.: Variability of isotope composition of precipitation in the southeastern Tibetan Plateau from the synoptic to seasonal time scale, Journal of Geophysical Research: Atmospheres, 125, e2019JD031751, 2020.

Sprenger, M., Herbstritt, B., and Weiler, M.: Established methods and new opportunities for pore water stable isotope analysis, Hydrological Processes, 29, 5174-5192, 2015.

Steen-Larsen, H. C., Masson-Delmotte, V., Sjolte, J., Johnsen, S. J., Vinther, B. M., Bréon, F. M., Clausen, H. B., Dahl-Jensen, D., Falourd, S., and Fettweis, X.: Understanding the climatic signal in the water stable isotope records from the NEEM shallow firn/ice cores in northwest Greenland, Journal of Geophysical Research Atmospheres, 116, 161-165, 2011.

Wassenaar, L., Hendry, M., Chostner, V., and Lis, G.: High resolution pore water δ2H and δ18O measurements by H2O (liquid)− H2O (vapor) equilibration laser spectroscopy, Environmental science & technology, 42, 9262-9267, 2008.

West, A. G., Goldsmith, G. R., Brooks, P. D., and Dawson, T. E.: Discrepancies between isotope

https://doi.org/10.5194/amt-2024-151
Preprint. Discussion started: 4 November 2024

ratio infrared spectroscopy and isotope ratio mass spectrometry for the stable isotope analysis of plant and soil waters, Rapid Communications in Mass Spectrometry, 24, 1948-1954, 2010.

West, J. B., Bowen, G. J., Dawson, T. E., and Tu, K. P.: Isoscapes: understanding movement, pattern, and process on Earth through isotope mapping, Springer, 2009.

Worden, J., Bowman, K., Noone, D., Beer, R., Clough, S., Eldering, A., Fisher, B., Goldman, A., Gunson, M., Herman, R., Kulawik, S. S., Lampel, M., Luo, M., Osterman, G., Rinsland, C., Rodgers, C., Sander, S., Shephard, M., and Worden, H.: Tropospheric emission spectrometer observations of the tropospheric HDO/H2O ratio: Estimation approach and characterization, Journal of Geophysical Research-Atmospheres, 111, 2006.

Yu, W., Tian, L., Ma, Y., Xu, B., and Qu, D.: Simultaneous monitoring of stable oxygen isotope composition in water vapour and precipitation over the central Tibetan Plateau, Atmospheric Chemistry and Physics, 15, 10251-10262, 2015.